Integrin αvβ3 and disulfide bonds play important roles in NGR-retargeted adenovirus transduction efficiency

Davor Nestić[a], Amela Hozić[b], Zlatko Brkljača[c], Ana Butorac[b], Kristijan Pazur[a], Betsy Jullienne[d], Mario Cindrić[b], Andreja Ambriović-Ristov[a#], Karim Benihoud[d#], Dragomira Majhen[a#*]

[a]Division of Molecular Biology, Ruđer Bošković Institute, 10000 Zagreb, Croatia

[b]Division of Molecular Medicine, Ruđer Bošković Institute, 10000 Zagreb, Croatia

[c]Division of Organic Chemistry and Biochemistry, Ruđer Bošković Institute, 10000, Zagreb, Croatia.

[d]Université Paris-Saclay, CNRS, Institut Gustave Roussy, Metabolic and systemic aspects of oncogenesis for new therapeutic approaches, 94805, Villejuif, France.

#corresponding authors

*inquiries should be directed to: Dragomira Majhen, Ruđer Bošković Institute, Bijenička cesta 54, 10000 Zagreb, Croatia, tel: +38514561145, fax: +38514561177, email: dmajhen@irb.hr

Word count: 6820 words

Table/figure count: 1 Table, 8 Figures

Abstract

Aims: AdFNGR and AdHNGR that have CNGRCVSGCAGRC peptide inserted into fiber or hexon protein, respectively, showed increased transduction of endothelial cells. In this study we investigated if cysteines within the CNGRCVSGCAGRC sequence inserted into Ad5 fiber or hexon protein form disulfide bond(s) and whether they play a role in retargeting potential of AdFNGR and AdHNGR.

Methods: Transduction efficiency of adenoviruses was done by counting infected cells under the microscope. Adenovirus attachment and internalization were measured by qPCR. Flow cytometry was used to evaluate the expression of CD13 and integrins. Gene knockdown was achieved by transfection of small interfering RNA. Mass spectrometry was used for determining disulfide bonds in adenovirus fiber and hexon protein. Molecular modeling was use to predict interaction of CNGRCVSGCAGRC peptide and CD13.

Key findings: AdFNGR and AdHNGR attach better to CD13 and/or αvβ3 integrin-positive cells than Adwt. Reducing disulfide bonds using DTT decreased transduction efficiency and attachment of both AdFNGR and AdHNGR. Cysteins from CNGRCVSGCAGRC peptide within AdHNGR do not form disulfide bonds. Knockdown of αvβ3 integrin reduced increased transduction efficiency of both AdFNGR and AdHNGR, while CD13 knockdown had no effect, indicating that retargeting properties of these viruses rely mainly on αvβ3 integrin expression.

Significance: Insertion site of NGR-containing peptides as well as NGR flanking residues are critical for receptor binding affinity/specificity and transduction efficiency of NGR retargeted adenoviral vectors.

Keywords

Adenovirus vector, NGR retargeting peptide, CD13, integrin

Introduction

The ability of NGR containing peptides to home specifically to tumor blood vessels was identified by *in vivo* selection of phage display libraries [1]. Initial assumption was that the receptor for the NGR peptides in tumor vasculature is aminopeptidase N (APN; CD13) [2], however NGR containing peptide can also target RGD-binding integrin(s). Under cellular condition NGR containing peptides are prone to non-enzymatic deamidation leading to the generation of aspartyl and isoaspartyl (DGR and isoDGR) derivatives [3]. Unlike NGR and DGR, isoDGR can efficiently mimic RGD in binding αvβ3 integrin. Spontaneous transition of NGR to isoDGR occurs also in fibronectin generating new αv integrin binding sites [4] thus highlighting the critical role of molecular scaffold on the biological properties of NGR/isoDGR peptides. Cyclic peptides mostly undergo NGR-to-isoDGR transition and CD13/integrin switching, whereas linear peptides mainly undergo degradation reactions which generate ring compounds unable to bind αvβ3 integrin, and small amount of isoDGR [5].

NGR peptides are used for ligand-directed targeted delivery of various drugs and particles to tumors or other tissues with an angiogenesis component [6, 7]. Both linear and cyclic NGR peptides have been used for tumor targeting, however, it has been shown that anti-tumor activity of cyclic was higher than that of linear, attributing this to the presence of disulfide bonds within NGR peptide [8]. Cyclic version of the NGR peptide complexed to the human TNF-α was evaluated in Phase III clinical trial in mesothelioma [9]. Besides for delivering different therapeutic compounds, NGR peptides have been used for cancer imaging [10] but also to retarget viral vectors like retrovirus [11], adeno-associated virus [12] and adenovirus [13, 14].

Adenoviruses (Ads) are intensively studied as vectors for tumor gene therapy and vaccination. Ad infection starts with virus binding to its primary receptor, followed by interaction of RGD sequence from penton base with αv integrins on cell surface allowing subsequent internalization of viral particle [15]. Vectors based on Ad serotype 5 require the coxsackie adenovirus receptor (CAR) for efficient infection and, hence, exhibit a tropism determined by the tissue distribution of the CAR expression. This leads to high transduction of non-target cells and low transduction of the target cells, problems that can be solved by Ad retargeting [16]. We have reported previously that Ad5NGR4C, containing CDCNGRCFC within potentially cyclic sequence, retargeted Ad5 mainly to CD13, while Ads containing linear NGR motifs without cysteines retargeted Ad5 mainly to αvβ3 integrin, albeit with a lower affinity [13]. By using mass spectrometry, we have demonstrated that the disulfide bond formed within RGD4C motif inserted into fiber protein of Ad5RGD4C is crucial for retargeting to αv-integrins [17].

AdFNGR and AdHNGR that have CNGRCVSGCAGRC peptide inserted into fiber or hexon protein, respectively, showed increased transduction of endothelial cells [14]. Until now, there has been no thorough investigation of how cysteines present in the CNGRCVSGCAGRC sequence influence retargeting potential of AdFNGR and AdHNGR. Therefor here we determined if cysteines within the CNGRCVSGCAGRC sequence form disulfide bond(s) and what is its/their role in retargeting potential of AdFNGR and AdHNGR.

Material and methods

Cell lines

HEK-293 (human embryonic kidney; ATCC CRL-1573), RD (human embryonal rhabdomyosarcoma; ATCC CCL-136), MDA-MB-435S (human melanoma; ATCC HTB-129) were purchased from the American Type Culture Collection (ATCC, Manassas, VA, USA) and maintained in DMEM medium. The SLK cell line, 9402 was obtained through the NIH AIDS Research and Reference Reagent Program, Division of AIDS, NIAID, NIH, from Dr JA Levy for Dr S Leventon-Kriss and were growth in RPMI 1640 medium. Cells were grown as a monolayer culture at 37ºC with 5% CO_2 in adequate medium supplemented with 10% fetal bovine serum.

Adenovirus vectors

All replication-deficient adenovirus vectors used in this study are based on adenovirus type 5 and have been previously described [14]. They were amplified in HEK-293 cells, banded in CsCl gradients and stored at -80ºC in aliquots. The virus particle concentration was measured by optical density according to the known protocol [18]. All viruses contain the *lacZ* reporter gene under the control of the human cytomegalovirus (CMV) immediate early promoter.

Determination of cell surface receptor expression by flow cytometry

Flow cytometry was used to analyze expression of integrin heterodimers αvβ3 and αvβ5, as well as CD13 on RD, SLK and MDA-MB-435S cell lines. Briefly, adherent cells were grown until 80% confluence, detached by trypsin and washed twice with PBS. Subsequently cells were incubated on ice with the following antibodies: anti-human CAR

MAb (clone RmcB, 05-644, Merck), anti-human αvβ3 integrin MAb (clone LM609, MAB1976, Merck), anti-human αvβ5 integrin MAb (clone P1F6, MAB1961, Merck), and anti-human CD13 MAb (clone WM15, sc-51522, Santa Cruz). The binding of these primary antibodies was revealed by using FITC-conjugated anti-mouse Ig antibody (polyclonal RUO, 554001, BD Bioscience) as secondary reagent.

Transduction efficiency

Transduction efficiency was assessed by β-galactosidase (β-gal) activity which was measured using a chemiluminescent assay (BD Biosciences Clontech, Palo Alto, CA, USA) or by X-Gal (5-bromo-4-chloro-3-indolyl-β-D-galactopyranoside) staining. In case of using chemiluminescent assay protein content was determined using the Bio-Rad Protein Assay (Bio-Rad Laboratories, Hercules, Marnes-la-Coquette, France). Results are expressed as relative light units per µg of protein. When using X-Gal staining the number of stained cells was counted under a light microscope. Cells were infected for 1 h with serial dilutions of Adwt, AdFNGR and AdHNGR normalized for identical amount of physical particles (pp) per milliliter. For experiments in which the effect of the reducing agent DTT on the biological functions of vector particles was examined, all Ads were incubated before infection with different concentrations of DTT (10 mM and 4 mM) for 1 h at 37ºC. Following the one-hour incubation with cells, viruses were removed and fresh medium was added. After 24 h β-galactosidase activity was determined [13].

Adenovirus binding and internalization measured by qPCR

Protocol used for determining binding and internalization of Ads was described previously [19]. Briefly, adherent cells were grown in 35-mm tissue culture dishes and Ads at the

multiplicity of infection (moi) of 1000 physical particles per cell (pp/cell) were added to cells and incubated for 1 h on ice. Unbound viruses were removed by washing the cells twice with cold trypsin and twice with cold PBS. To measure binding, cells were then harvested with a cell scraper and pelleted by centrifugation. To measure internalization cells were transferred at 37ºC for 1 h, washed twice with cold trypsin, trypsinized at 37ºC and, after addition of PBS, immediately pelleted by centrifugation. Total DNA was extracted from cell pellets using DNeasy kit (Qiagen) and 100 ng was used to quantify viral DNA. Adenovirus binding and internalization were quantified by qPCR using a target sequence within the gene encoding hexon. Normalization was done towards GAPDH gene [19].

Gene knockdown achieved by transfection of small interfering RNA (siRNA)

To knockdown specific receptors, we used the following Ambion Silencer Select predesigned siRNAs: CD13 siRNA (ID# s683) and β3 integrin subunit siRNA (ID# s7581). As a negative control we used non-targeting control siRNA #1 (Ambion). Cells were transfected at a confluence of about 50% using Lipofectamine RNAiMax reagent (Invitrogen) according to manufacturer's protocol. Final concentration of specific siRNAs was 50 nM. Cells were then used in flow cytometry experiments to determine the knockdown efficiency, or in transduction and binding experiments to measure transgene expression and viral DNA level.

Ultra performance liquid chromatography–mass spectrometry-to-the-E (UPLC–MSE) analysis

Mass spectrometry was performed using purified AdFNGR and AdHNGR viruses. Purified viruses were incubated with *Rapi*Gest solution in final concentration of 0.1% and treated with or without DTT for 30 min on 60ºC. Subsequently, trypsin hydrolysis was performed at 37 °C for 18 h. Then, peptides were separated on a Waters nanoAcquity UPLC system with flow rate 1 µL/min by using the Acquity UPLC column BEH130 C18 (100 µm x 100 mm, Waters, Milford, MA, USA) and pre-column 2G-V/M Trap 5 µm Symmetry C18 (180 µm x 20 mm, Waters, Milford, MA, USA) with flow rate 15 µL/min to desalt samples prior separation. A 60-min gradient was used for the separation of AdHNGR peptides and a 75-min one for the AdFNGR peptides. Solvent A consisted of 0.1% formic acid in water (v/v) and solvent B of 0.1% formic acid in 95% acetonitrile (v/v). The injection volume was 2 µL. UPLC system was coupled to the ESI-qTOF SYNAPT G2-Si (resolution mode of operation) mass spectrometer (Waters, Milford, MA, USA). The instrument parameters were set using the Mass Lynx software version 4.1. SCN902 (Waters, Milford, MA, USA). LC–MS data was collected in low energy and elevated energy (MSE) mode of acquisition. Parameters were set as follows: positive ion mode, desolvation nitrogen flow 0.6 Bar with a temperature of 150°C, the capillary voltage 4.0 kV, and the cone voltage 40 V. The spectral acquisition time was 1 s. MS acquisition was set to 50 – 3000 Da. In low energy MS mode, data was collected at constant collision energy of 4 eV and in elevated energy MS mode the collision energy was ramped from 20 to 45 eV during each 1 s data collection cycle. The mass accuracy of the raw data was corrected infusing leucine enkephalin (1 ng/µL, 0.4 µL/min flow rate, 556.2771 Da $[M + H]^+$) into the mass spectrometer as a lock mass during sample analysis. The raw data were processed with ProteinLynx Global Server (PLGS; version 3.0.1; Waters). Peak lists were generated after deisotoping and deconvolution. Databank search query (PLGS workflow) was carried out as follows:

peptide and fragment tolerances were set to automatic, three fragment ion matches per peptide, seven fragment ions per protein. Primary digest reagent was trypsin with two missed cleavages allowed. Following variable modifications were allowed: oxidation M, deamidation NQ and dehydration ST. MSE data were searched against AdFNGR and AdHNGR sequences, respectively.

Molecular modeling

We performed all-atom molecular dynamics MD simulations of Porcine Aminopeptidase N protein together with tridecapeptide (amino acid sequence CNGRCVSGCAGRC, capped with acetyl and N-methyl amide groups on N- and C-termini, respectively) in water environment. The initial protein structure was obtained from Protein Data Bank (code 4OU3). Subsequently, the protein and the polypeptide were parameterized using AMBER ff14SB force field [20], with the zinc ion present in the groove of the protein and the amino acids coordinating it (R325, R344 and E416) being parameterized using extended 4-ligand model [21]. The protein structure was immersed in rectangular water box containing 80000 water molecules (box dimensions ≈ 13.7 nm x 13.7 nm x 13.7 nm). To neutralize the net charge of the simulation boxes 28 sodium ions were added. To describe water molecules, we used standard TIP3P water model, with present ions described using parameters developed by Cheatham III et al. [22] (ion parameters used in AMBER force fields).

The polypeptide was placed inside the pocket of the protein (see Figure 7) and thus prepared system was subjected to the minimization/equilibration procedure. In this respect, the simulation box was first minimized using steepest descent algorithm (5000 steps), and was subsequently relaxed for the duration of 2 ns at T = 310 K (NVT ensemble)

with the time step of 2 fs, where we used Berendsen thermostat (time constant for temperature coupling set at 1 ps), and where position restraints on all heavy atoms (all atoms other than hydrogens) of the protein and polypeptide were imposed (1000 kJ mol^{-1} nm^{-2}). After the initial relaxation in canonical ensemble we equilibrated systems at T = 310 K (NPT ensemble), where we again used Berendsen thermostat to maintain temperature (time constant for temperature coupling set at 1 ps) and Berendsen barostat to maintain constant pressure of 1 bar (time constant for pressure coupling set to 5.0 ps) for 5 ns with the time step of 2 fs with weak position restraints again applied on the equivalent set of atoms as aforementioned (200 kJ mol^{-1} nm^{-2}). Finally, we propagated production runs in the duration of 100 ns. Production simulations of all prepared systems were propagated in NPT ensemble without any restraints, with Nose-Hoover thermostat incorporated to maintain temperature at T = 310 K (time constant for temperature coupling of 1 ps), whereas Parrinello-Rahman barostat was used to maintain constant pressure of 1 bar (time constant for pressure coupling set to 5.0 ps). All aforementioned explicit simulations were performed with periodic boundary conditions in all three directions, with long-range electrostatic interactions beyond a 1.2 nm cutoff taken into account via the particle mesh Ewald method [23]. All MD simulations in this study were conducted using GROMACS 2018 [24].

Statistical analysis

Each experiment was repeated at least three times unless otherwise noted. The data were analyzed by the unpaired Student's t-test and expressed as means ± standard deviation (SD). Data were considered statistically significant at a P-value < 0.05.

Results

AdFNGR and AdHNGR bind and transduce better CD13 and/or αvβ3 integrin-positive cells than Adwt

In our previous work we constructed two NGR-retargeted Ad5 by inserting a NGR-containing peptide into either fiber (AdFNGR) or hexon (AdHNGR) protein and showed that the presence of NGR motif allows better transduction of CD13- and/or αv integrin-positive cells. We also reported increased binding of two vectors mutated in the RGD motif of penton base, AdΔRGD–FNGR and AdΔRGD–HNGR, to immobilized αvβ3 integrin indicating that besides CD13, αvβ3 integrin could be a receptor for AdFNGR and AdHNGR [14]. Here we confirmed our previously obtained data [14], i.e. increased transduction efficiency of AdFNGR and AdHNGR in MDA-MB-435S, RD and SLK cells, compared to Adwt (Fig. 1A, B). RD cells express high levels of CD13 and low levels of αvβ3 integrin, MDA-MB-435S cells express high levels of αvβ3 integrin, but do not express CD13 while SLK cells express high levels of CD13 and αvβ3 integrin. These cell lines were selected because they are CAR negative to prevent CAR-mediated transduction, since viruses used in this study were not ablated for CAR binding (Table 1). Therefore, both increased transduction efficiency of AdFNGR and AdHNGR as well as differences thereof compared to Adwt (displaying a wild-type capsid), observed in MDA-MB-435S, RD and SLK cells could be attributed to cell surface expression of CD13 and/or αvβ3 integrin.

Table 1. Cell surface expression of CAR, CD13, αvβ3 and αvβ5 integrins.

Cells	CD13	CAR	αvβ3	αvβ5	Ref.
MDA-MB-435S	**-**	**-**	**+**	**+**	[14, 25]
RD	**+**	**-**	**±**	**±**	[13, 25]
SLK	**++**	**-**	**++**	**+**	[14]; this work

Assignment of expression levels: **−**: negative (compared to isotype control); ±, weak: below 50% of positive cells, +: positive, more than 50% of positive cells, ++: 100% of positive cells.

Next, we sought to determine the role of binding/binding and internalization in increased transduction efficiency of NGR-retargeted Ad5. Compared to Adwt, both AdFNGR and AdHNGR show increased binding and internalization in all three cell lines, MDA-MB-435S; RD and SLK (Fig. 1C, D), in accordance with data obtained for transduction experiments. Interestingly, in MDA-MB-435S cells AdHNGR has higher binding and internalization than AdFNGR, but lower transduction efficiency. It is possible that the receptor for AdHNGR on MDA-MB-435S, or modification of the hexon itself, provides good binding and internalization but less successful trafficking toward nucleus.

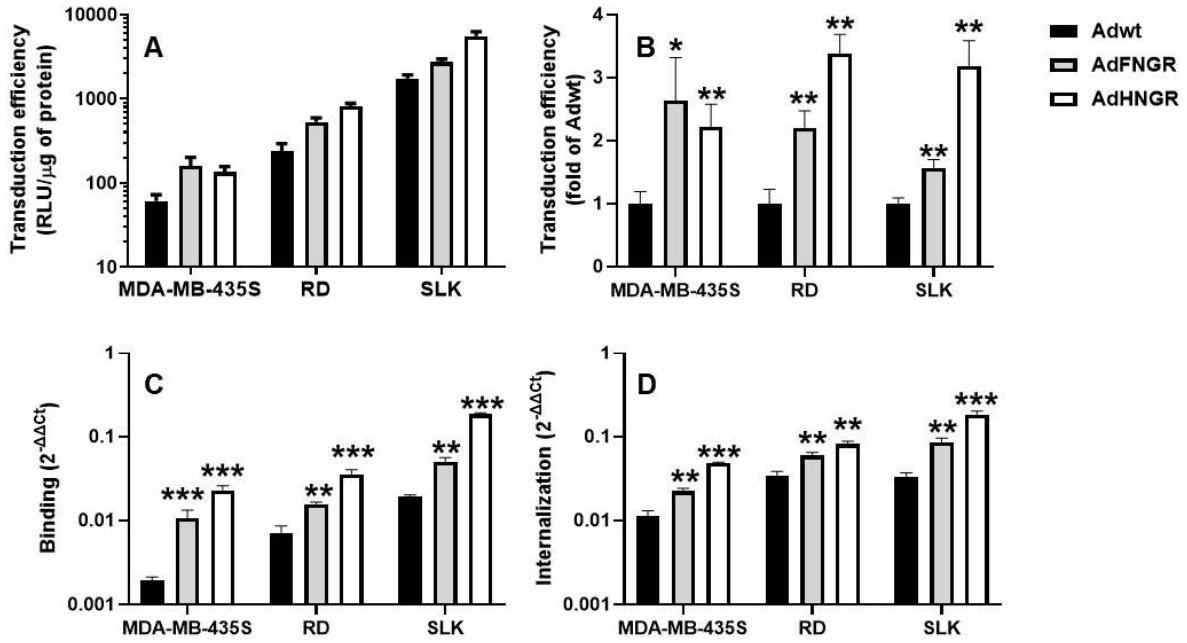

Figure 1. Transduction efficiency, binding and internalization of Adwt, AdFNGR and AdHNGR in CD13- and/or αvβ3 integrin-positive cells. (A, B) For transduction, cells were infected for 1 h with serial dilutions of Ads normalized for identical amount of physical particles (pp) per milliliter. Viruses were then removed and fresh medium was added. Transduction efficiency was assessed by β-galactosidase (β-gal) activity. Absolute transduction efficiency (A) and transduction efficiency relative to Adwt (B) are shown. - For (C) binding and (D) internalization, cells were incubated with Ads at the multiplicity of infection (moi) 1000 pp/cell for 1 h on ice. To measure binding, unbound viruses were removed and cells were scraped off and pelleted. To measure internalization, unbound viruses were removed and cells were incubated at 37°C for 1 h, trypsinized and pelleted. Total DNA was extracted from cell pellets and used for quantification of viral DNA by qPCR using hexon gene as a target sequence and GAPDH gene for normalization. The results ± SD of one experiment out of three independent experiments with similar results are

shown. Statistical differences relative to cells infected with Adwt are shown (** P ≤ 0.05, ** P ≤ 0.01, *** P ≤ 0.001*).

Reduction of disulfide bonds decreases binding and transduction efficiency of AdFNGR and AdHNGR

Using pretreatment with DTT, we previously hypothesized the existence of a disulfide bond within RGD4C peptide inserted in the HI loop of Ad5 fiber which was unequivocally demonstrated by mass spectrometry [17]. Therefore, the same protocol was used to investigate whether cysteins within CNGRCVSGCAGRC peptide inserted into Ad5 fiber or hexon form disulfide bond(s) crucial for increased transduction efficiency of NGR-retargeted Ads. Briefly, AdFNGR and AdHNGR were mock-treated or treated with DTT prior to cell infection and both cell transduction efficiency and binding were assessed. DTT treatment significantly decreased transduction efficiency of AdFNGR in all three cell lines, in a dose-dependent way while it had no effect on Adwt (Fig. 2, left panel). The fact that DTT had no influence on transduction efficiency of non-retargeted Ad5 was confirmed also in our previous research [13]. The decrease in transduction efficiency of AdHNGR at both DTT concentrations (4 and 10 mM) was observed in RD and SLK cells, i.e. CD13- and αvβ3 integrin-positive cell lines, while effect in αvβ3 integrin-positive MDA-MB-435S cells was seen only at the higher DTT concentration (Fig. 2, left panel). In this latter cell line, the decrease in transduction efficiency after reducing disulfide bonds was more pronounced for AdFNGR than AdHNGR. Together, this suggests the presence of a disulfide bond(s) in CNGRCVSGCAGRC sequence inserted into the fiber or hexon protein that influences retargeting potential of AdFNGR and AdHNGR. Interestingly, DTT

treatment decreased AdFNGR transduction efficiency almost to the level observed for Adwt, while AdHNGR upon DTT treatment still maintained increased transduction compared to Adwt.

Transduction efficiency of adenoviral vectors depends on several steps preceding entry of adenovirus DNA into nucleus, with virus binding being one of them. In order to determine whether reducing disulfide bonds in NGR-retargeted Ad5 influences their binding efficiency we measured the amount of viral DNA found in cell lines incubated with NGR-retargeted viruses untreated or treated with DTT. DTT treatment significantly reduced binding of AdFNGR and AdHNGR on all examined cell lines (RD, MDA-MB-435S and SLK) (Fig. 2, right panel). Similarly, as observed for transduction efficiency, DTT treatment completely abolished increased binding of AdFNGR in all three cell lines while increased binding of AdHNGR was only partially abrogated.

Together, these results suggest the existence of disulfide bond(s) between cysteines flanking NGR sequence inserted into AdFNGR and AdHNGR that are crucial for their retargeting potential.

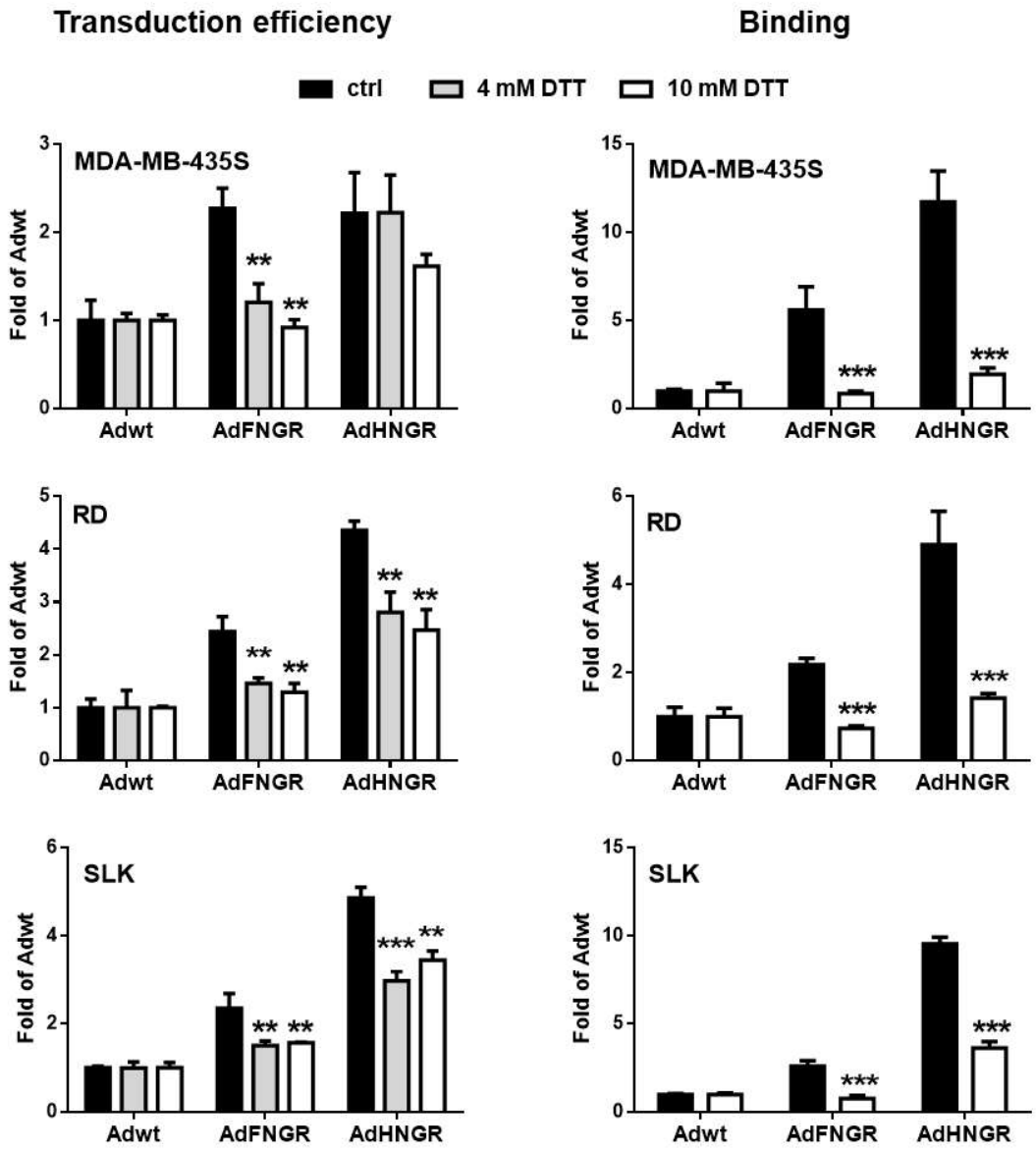

Figure 2. Transduction efficiency and binding of Adwt, AdFNGR and AdHNGR in CD13- and/or αvβ3 integrin-positive cells after virus treatment with DTT. Ads were incubated with or without DTT (10 and 4 mM) for 1 h at 37°C prior to incubation with cells. For transduction, cells were infected for 1 h with serial dilutions of Ads normalized for identical amount of physical particles (pp) per milliliter. Then, unbound viruses were removed and fresh medium was added. 24 h later, cells were fixed and stained for β-

galactosidase activity (left panel). For binding (right panel), cells were incubated with Ads at the multiplicity of infection (moi) of 1000 pp/cell for 1 h on ice. After unbound viruses were removed, total DNA was extracted from cell pellets and used for quantification of viral DNA by qPCR using hexon gene as a target sequence and GAPDH gene for normalization. For each DTT concentrations the results are presented as fold of Adwt ± SD. The results are representative of three independent experiments with similar results. Statistical differences relative to cells infected with Adwt are shown (** $P \leq 0.05$, ** $P \leq 0.01$, *** $P \leq 0.001$*).

Cysteins from CNGRCVSGCAGRC peptide within AdHNGR do not form disulfide bonds

Next, we sought to determine the number and position of disulfide bond(s) within CNGRCVSGCAGRC sequence inserted in AdFNGR and AdHNGR. In order to do this, we analyzed by mass spectrometry fiber or hexon protein from purified AdFNGR or AdHNGR, respectively. Fragment ion mass spectrum (MSE) of the deamidated triply protonated peptide QQNGKLESQVEMQFFCNGRCVSGCAGR (m/z [M+3H]3+ 993.1111) with identified fragment ions containing C_{268}NGRC_{272}VSGC_{276}AGRC_{280} from AdHNGR is shown on Figure 3. Based on the mass spectrometry results, we can conclude that there are no disulfide bonds between the thiol groups of the cysteines from the CNGRCVSGCAGRC amino acid sequence inserted into the AdHNGR hexon protein. We previously observed similar results with another retargeting peptide, αvβ3 targeting CRGDCVSGCAGRC inserted into the hexon protein of Ad5HCRGDC (data not shown), leading us to hypothesize that hexon protein as an insertion moiety does not allow

formation of disulfide bonds within CNGRCVSGCAGRC or CRGDCVSGCAGRC targeting sequences. In addition, none of other cysteines present into hexon protein can form disulfide bonds. This is unexpected result since pretreatment with DTT clearly showed reduction of AdHNGR binding, internalisation and transduction efficiency. However, mass spectrometry data would not detect possible intermolecular / interviral disulfide bonds which might result in a such outcome (see details in discussion section). Unfortunately, with this experimental setting we were not able to detect mass spectrum of the fiber protein.

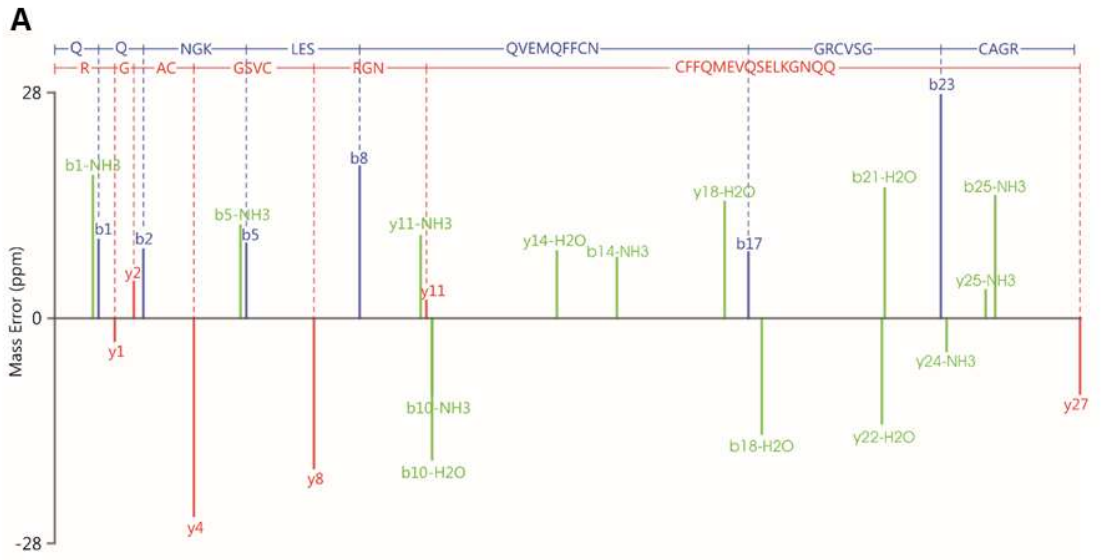

B

MATPSMMPQWSYMHISGQDASEYLSPGLVQFARATETYFSLNNKFRNPTVAPTHDVTTDRSQRLTLRFIPVDREDTAYSYKARFTLAVGDNRVL
DMASTYFDIRGVLDRGPTFKPYSGTAYNALAPKGAPNPC$_{133}$EWDEAATALEINLEEEDDDNEDEVDEQAEQQKTHVFGQAPYSGINITKEGIQIG
VEGQTPKYADKTFQPEPQIGESQWYETEINHAAGRVLKKTTPMKPC$_{233}$YGSYAKPTNENGGQGILVKQQNGKLESQVEMQFFC$_{268}$NGRC$_{272}$VS
GC$_{276}$AGRC$_{280}$KVVLYSEDVDIETPDTHISYMPTIKEGNSRELMGQQSMPNRPNYIAFRDNFIGLMYYNSTGNMGVLAGQASQLNAVVDLQDRN
TELSYQLLLDSIGDRTRYFSMWNQAVDSYDPDVRIIENHGTEDELPNYC$_{412}$FPLGGVINTETLTKVKPKTGQENGWEKDATEFSDKNEIRVGNNFA
MEINLNANLWRNFLYSNIALYLPDKLKYSPSNVKISDNPNTYDYMNKRVVAPGLVDC$_{514}$YINLGARWSLDYMDNVNPFNHHRNAGLRYRSMLL
GNGRYVPFHIQVPQKFFAIKNLLLLPGSYTYEWNFRKDVNMVLQSSLGNDLRVDGASIKFDSIC$_{612}$LYATFFPMAHNTASTLEAMLRNDTNDQSF
NDYLSAANMLYPIPANATNVPISIPSRNWAAFRGWAFTRLKTKETPSLGSGYDPYYTYSGSIPYLDGTFYLNHTFKKVAITFDSSVSWPGNDRLLTP
NEFEIKRSVDGEGYNVAQC$_{757}$NMTKDWFLVQMLANYNIGYQGFYIPESYKDRMYSFFRNFQPMSRQVVDDTKYKDYQQVGILHQHNNSGFVG
YLAPTMREGQAYPANFPYPLIGKTAVDSITQKKFLC$_{864}$DRTLWRIPFSSNFMSMGALTDLGQNLLYANSAHALDMTFEVDPMDEPTLLYVLFEVF
DVVRVHQPHRGVIETVYLRTPFSAGNATT

C

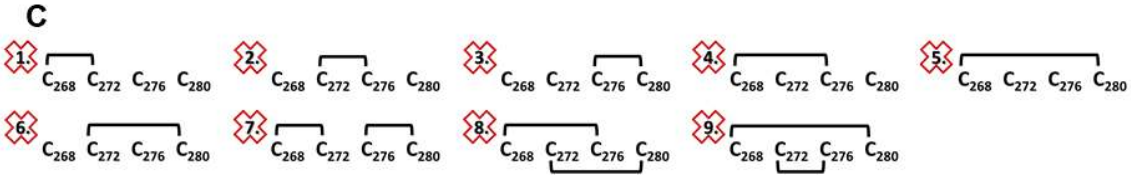

Figure 3. Mass spectrometry analysis of AdHNGR hexon protein. Purified AdHNGR was digested with trypsin and then peptide samples were separated on a Waters nanoAcquity UPLC system coupled to the ESI-qTOF SYNAPT G2-Si mass spectrometer. (A) Mass spectrum (Product ion/High energy) of QQNGKLESQVEMQFFCNGRCVSGCAGR peptide with deamidations on Q(2) and N(3) derived from hexon protein acquired in MSE mode on a Synapt G2-Si as analyzed by PLGS software with an ion score of 7.0, precursor RMS error of 3.4 ppm, and the product RMS error of 11.4 ppm is shown. Annotations are coded as y-ions (red), b-ions (blue), and neutral losses of H2O and NH3 (green). (B) The amino acid sequence of hexon protein from AdHNGR displaying the inserted NGR motif (bold), the detected peptide containing CNGRCVSGCAGR (green), and other cysteines and their positions outside NGR motif (blue) is shown. (C) Red indicates disulfide bonds that are certainly absent.

Knockdown of αvβ3 integrin decreases transduction efficiency of NGR-retargeted Ad

In order to determine whether inserting NGR-retargeting peptide in Ad5 fiber or hexon gives preference to CD13 or αvβ3 integrin we measured transduction efficiency of AdFNGR and AdHNGR in MDA-MB-435S, RD and SLK cells after CD13 or αvβ3 integrin knockdown using siRNAs specific for CD13 or integrin subunit β3. Since integrins are heterodimers composed of α and β subunits, reduced expression of one specific heterodimer is achievable by transfection of siRNA specific for a subunit which is not shared with other integrin heterodimers. In the case of integrin αvβ3 this can be realized in many cell lines by transfection of integrin β3 specific siRNA. However, in some cell lines

unexpected integrin crosstalk effect i.e. modulation of some other integrin expression may occur [26, 27]. The successful knockdown of CD13 or αvβ3 integrin in MDA-MB-435S, RD and/or SLK cells was confirmed by flow cytometry as shown in figure 4.

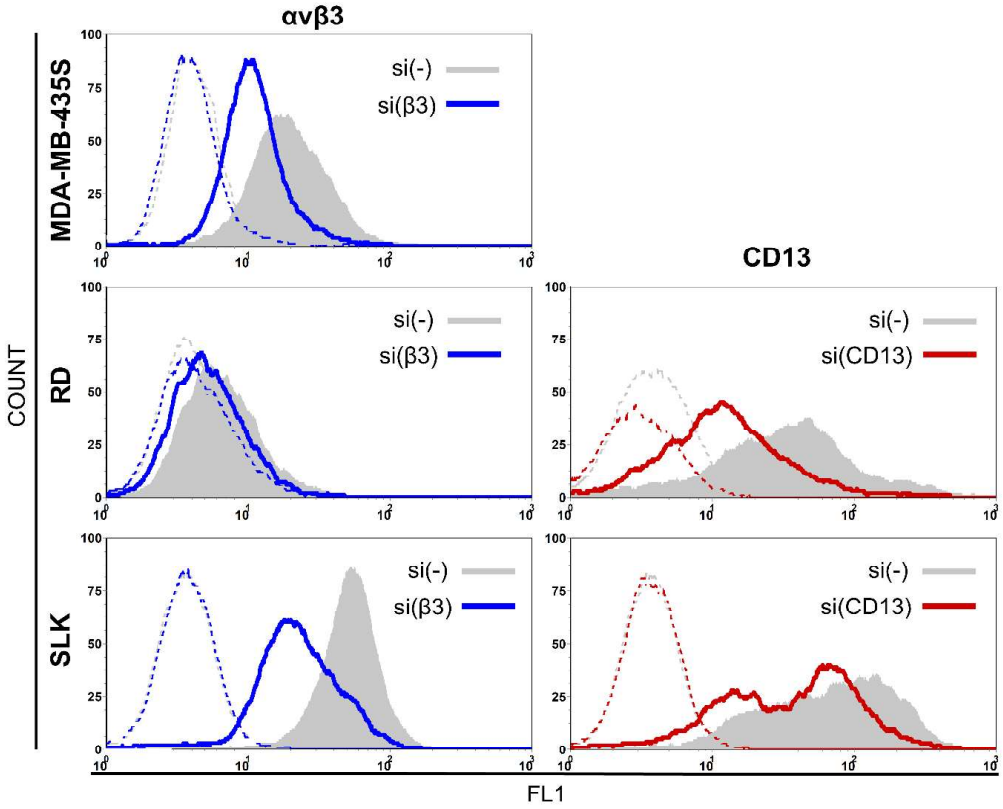

Figure 4. Cell surface expression of CD13 and αvβ3 integrin following cell transfection by specific siRNA. Cells were transfected with control or specific siRNA (50 nM) and 48 h later surface expression of CD13 and αvβ3 integrin was determined by flow cytometry. Shaded histograms show expression of CD13 or αvβ3 integrin in control cells transfected with nonspecific siRNA, si(-). Bold blue line presents expression of αvβ3 integrin after si(β3), bold red line presents expression of CD13 after si(CD13). Staining with isotype-matched antibody as a negative control is presented with dotted lines in

corresponding colors. The representative data of three independent experiments which yielded similar results are shown.

Decreased expression of αvβ3 integrin due to β3 integrin knockdown completely abolished increased transduction efficiency of both AdFNGR and AdHNGR in RD cell line and reduced increased transduction efficiency of AdFNGR compared to Adwt in MDA-MB-435S cell line (Fig. 5). Conversely, decreased expression of αvβ3 integrin had no effect on transduction efficiency of AdHNGR in MDA-MB-435S or SLK cell lines nor of the one of AdFNGR in SLK cell line. Contrary to αvβ3 integrin, CD13 knockdown did not have any effect on transduction efficiency of AdFNGR or AdHNGR in RD or AdHNGR in SLK cells. We did observe small decrease in AdFNGR transduction in SLK cell after CD13 knockdown. Of note, since MDA-MB-435S cells are CD13 negative, we did not analyse the effect of CD13 knockdown on transduction efficiency of NGR-retargeted Ad5.

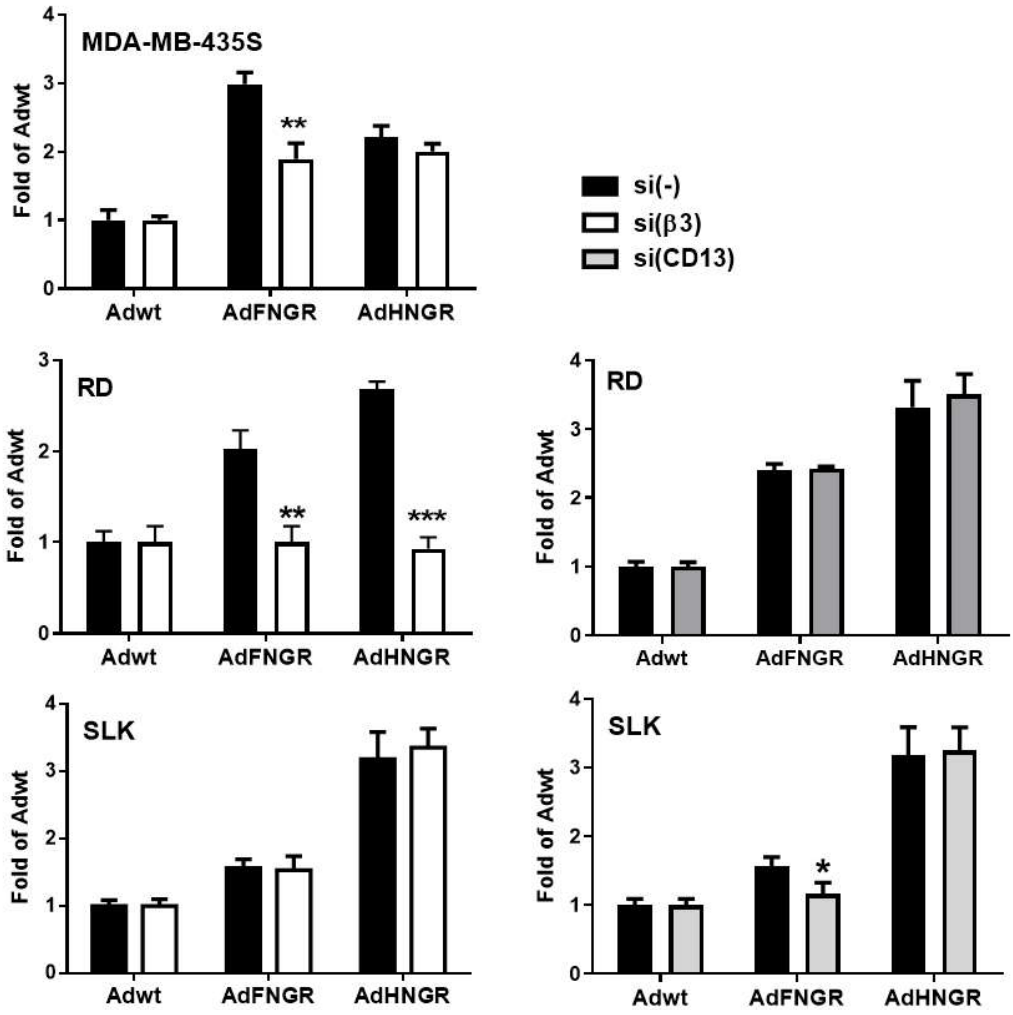

Figure 5. Transduction efficiency of Adwt, AdFNGR and AdHNGR in cells after knockdown of either CD13 or αvβ3 integrin. Cells were transfected with control (scramble) or specific siRNA (50 nM) and 24 h later cells were infected for 1 h with serial dilutions of Ads (normalized for identical amount of physical particles per milliliter). Viruses were then removed and fresh medium was added. After 24h, cells were fixed and stained for β-galactosidase activity. The results expressed as fold of Adwt ± SD are representative of three independent experiments with similar results. Statistical differences relative to cells transfected with si(-) are shown (*$P \leq 0.05$, **$P \leq 0.01$, ***$P \leq 0.001$).

Decreased expression of αvβ3 integrin due to β3 integrin knockdown reduced transduction efficiency of NGR-retargeted Ad5 in RD and MDA-MB-435S cell lines. Therefore, we decided to determine the role of αvβ3 integrin in NGR-retargeted Ad5 cell binding / entry. Decreased expression of αvβ3 integrin in MDA-MB-435S cell line (αvβ3 integrin-positive, CD13-negative), slightly, but significantly, decreased binding of Adwt, AdFNGR and AdHNGR. Knockdown of αvβ3 integrin in RD cell line (CD13 positive, low expression of αvβ3) decreased binding of Adwt, but increased binding of AdFNGR and AdHNGR (Fig. 6). This increased binding did not correlate with the decreased transduction efficiency that we observed in RD after decreased expression of αvβ3 integrin. Knockdown of CD13 had no influence on AdFNGR and AdHNGR binding, neither to RD nor to SLK cells. However, we did observe increased binding of Adwt in SLK indicating that knockdown of CD13 could have changed expression or availability of other molecules involved in Ad5 binding. All together we can conclude that αvβ3 integrin is important for increased transduction efficiency for both AdFNGR and AdHNGR, while in this experimental set up CD13 did not prove to be essential.

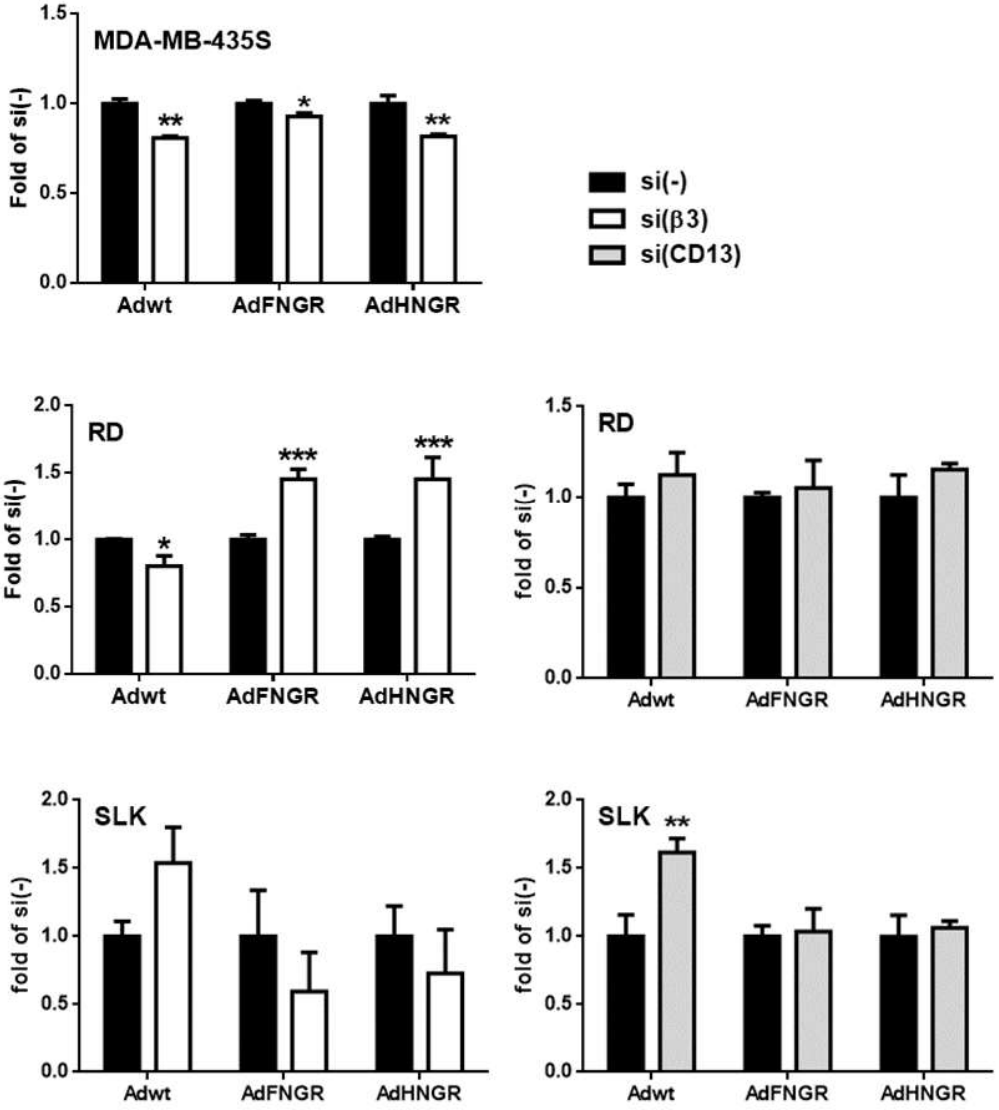

Figure 6. Binding of Adwt, AdFNGR and AdHNGR to cells after knockdown of αvβ3 integrin or CD13. Cells were transfected with control (si(-)) or specific (si(β3) or si(CD13)) siRNA (50 nM) and 24 h later cells were incubated with Ads at moi of 1000 pp/cell for 1 h on ice. After removal of unbound viruses, total cell DNA was used for quantification of viral DNA by qPCR using hexon gene as a target sequence and GAPDH gene for normalization. The results are presented as fold si(-) ± SD of control (cells transfected with scrambled siRNA). The results presented are representative of three independent

experiments with similar results. Statistical differences relative to si(-)-transfected cells are shown (* $P \leq 0.05$, ** $P \leq 0.01$, *** $P \leq 0.001$).

Interaction of CNGRCVSGCAGRC peptide with CD13

To examine if CNGRCVSGCAGRC peptide as such can dock to CD13 we performed all-atom molecular dynamics (MD) simulations of porcine CD13 protein together with capped tridecapeptide (CNGRCVSGCAGRC, see Molecular modeling section) in water environment, whereby we investigated the interaction of the small polypeptide inside the pocket of the porcine CD13. Based on the obtained molecular modeling results, we find that, from the perspective of the internal conformational phase space, NGR peptide shows strong propensity toward “U-turn” conformations (Fig. 8A, B), with virtually all conformations the polypeptide possesses inside the protein pocket being of the aforementioned type. On the other hand, the peptide exhibits interactions with amino acids situated in the vicinity of the CD13 active site (Fig. 8C) and interestingly, strongly interacts via hydrogen bonds with the helical domain H of the protein, thus inducing the conformational change in the protein whereby the helical domain H shifts toward the pocket of the protein (Fig. 8D). To the best of our knowledge, this is the first molecular model presenting interaction of CNGRCVSGCAGRC peptide and CD13.

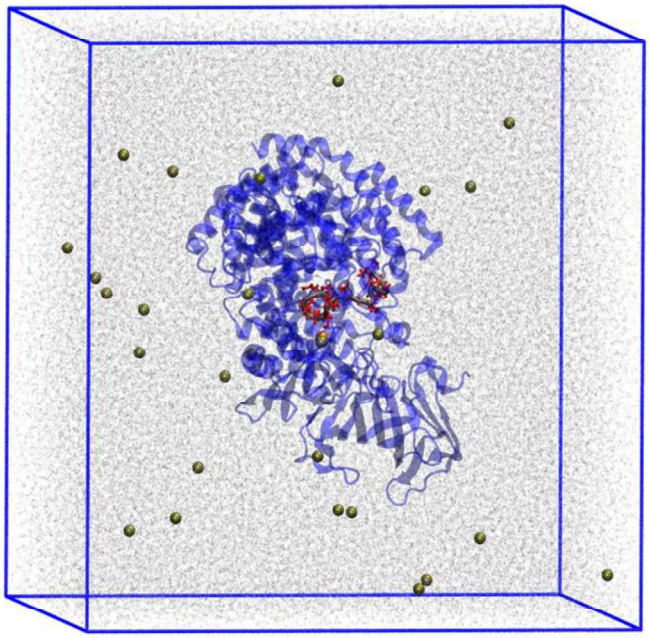

Figure 7. Snapshot of the entire simulated system (simulation box). CD13 is shown in blue transparent color, CNGRCVSGCAGRC polypeptide is shown in red and gray (backbone), zinc ion is shown in orange, while sodium ions are presented in dark yellow. Water is presented in the ghost mode (pale gray color) for better visibility. Snapshot is obtained using VMD software package [28].

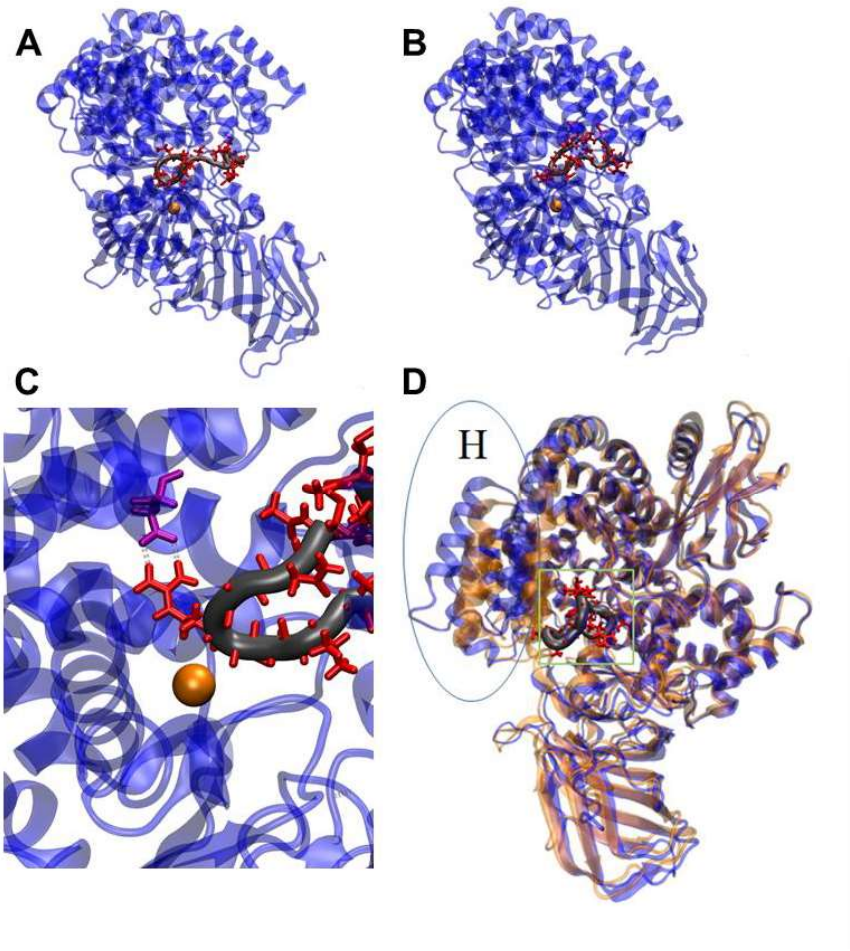

Figure 8. Interaction model of CNGRCVSGCAGRC peptide with CD13. (A) starting configuration of the polypeptide and (B) configuration after 80 ns of the simulation. During the course of the simulation, polypeptide shows the propensity toward “U-turn” (U-turn like) conformations. (C) Interaction of CD13 and CNGRCVSGCAGRC polypeptide in the vicinity of the CD13 active site (close to the zinc ion shown in orange) through the salt bridge formed between R4 from the polypeptide and D372 from the protein (shown in purple). (D) Interaction of CNGRCVSGCAGRC polypeptide with the helical domain H (highlighted in blue ellipse) of CD13 via hydrogen bonds induced the conformational change in the protein, whereby the helical domain H shifts toward the pocket of the protein.

Blue and orange protein conformations represent the beginning and the end of 100 ns long MD simulation, respectively. Possible penetration site for the polypeptide is denoted by green square.

Discussion

In this study we investigated if cysteines within the CNGRCVSGCAGRC sequence inserted into Ad5 fiber or hexon protein form (a) disulfide bond(s) and what is its/their role in retargeting potential of AdFNGR and AdHNGR. DTT treatment significantly decreased transduction efficiency and binding of both AdFNGR and AdHNGR suggesting there might be at least one disulfide bond present within CNGRCVSGCAGRC sequence or between these sequences located on different viral particles in the viral preparation, which influences retargeting potential of AdFNGR and AdHNGR. Since we also showed that decreased expression of αvβ3 integrin reduced increased transduction efficiency of AdFNGR and AdHNGR, while CD13 knockdown had less notable effect, we suggest that retargeting properties of these viruses rely mainly on αvβ3 integrin expression.

The role of disulfide bonds in retargeting potential toward αvβ3 integrin was previously shown for Ad5RGD4C, an Ad5 with inserted $C_{547}DC_{549}RGDC_{553}FC_{555}$ motif in the fiber protein [17]. Here, by using the same approach, we analyzed the fiber protein from purified AdFNGR and the hexon protein from purified AdHNGR. Our MS data revealed that none of the cysteines from $C_{268}NGRC_{272}VSGC_{276}AGRC_{280}$ peptide within AdHNGR hexon protein is engaged in disulfide bonds. We observed the same with CRGDCVSGCAGRC, αvβ3 targeting peptide, inserted into the hexon protein of Ad5HCRGDC (data not shown),

leading us to hypothesize that hexon protein as an insertion moiety does not allow circularization of CNGRCVSGCAGRC or CRGDCVSGCAGRC targeting sequences, therefore leaving NGR sequence of AdHNGR in the linear conformation.

Lack of disulphide bonds in hexon protein of AdHNGR observed by mass spectrometry does not corroborate our data obtained after DTT treatment, thus one can ask why DTT treatment reduce binding, internalization and transduction efficiency of AdHNGR if there are no disulphide bonds in hexon protein. The first hypothesis explaining these results is differential tendency of cyclic or linear NGR sequences to deamidation. In our experiments we used DTT for reducing possible disulfide bonds. At pH > 7 DTT treatment can increase the rate of deamidation of asparagine [29]. In our mass spectrometry results many detected NGR-containing peptides of AdHNGR, i.e. linear form of NGR peptide, have deamidation of asparagine as modification, namely transition of N to D. Hence, DTT-treated AdHNGR could lose affinity and specificity for all integrins, except in the case of α-aminogroup acetylation, whose detection was out of a scope of this study. The second possibility is that free thiol groups of cysteine residues from one AdHNGR virus particle interact with free thiol groups of cysteine residues from another virus particle hence creating agglomerates of AdHNGR. In such a setting binding of one agglomerate brings into the cell more than one particle. DTT treatment separates agglomerates into single particles, thus one binding event brings into the cell only one virus particle resulting in decreased transduction efficiency of DTT-treated AdHNGR.

By performing mass spectrometry analysis on purified virus we were not able to determine mass spectrum of fiber protein from AdFNGR. We assume that this is due to the low amount of fiber protein within viral particles, namely there are only 36 copies of fiber

protein per virus. Even though we cannot neither confirm nor exclude that cysteins from the $\underline{C}_{539}$NGR$\underline{C}_{543}$VSG$\underline{C}_{547}$AGR$\underline{C}_{551}$ sequence inserted into the fiber protein of AdFNGR form the disulfide bonds, the results obtained for binding and transduction efficiency after DTT treatment prompt us to speculate that at least one disulfide bond is present, either within CNGRCVSGCAGRC sequence or between these sequences positioned on different viral particles within the viral preparation.

Both CD13 and αvβ3 integrin allow increased transduction efficiency of AdFNGR and AdHNGR. Which of those two receptors is more important for retargeting potential and what is the role of different adenovirus molecular scaffolds, namely fiber and hexon, on peptide retargeting properties has not been investigated so far. Decreased expression of αvβ3 integrin completely abolished increased transduction efficiency of AdFNGR on MDA-MB-435S and RD cell line, indicating that AdFNGR is mainly retargeted toward αvβ3 integrin. Based on our results obtained after DTT treatment we believe that NGR sequence in AdFNGR is in cyclic form which can undergo NGR-to-isoDGR change and subsequently switch from CD13 to αvβ3 integrin binding. Decreased expression of αvβ3 integrin in MDA-MB-435S or SLK did not change transduction efficiency of AdHNGR, suggesting that linear conformation of NGR sequence in AdHNGR targets this virus towards some other integrins. Retargeting potential of NGR modification in the hexon towards other integrins was also described in our previous work where we unraveled a binding of AdΔRGD–HNGR to α5β1 integrin [14]. The discrepancy observed between binding and transduction efficiency of AdFNGR and AdHNGR in RD cell after knockdown of αvβ3 integrin could be a consequence of integrin crosstalk, a mechanism by which a change in the expression of a certain integrin subunit may interfere with the expression

and/or activation of other integrin subunit(s) in the very same cell [27]. In our previous work we saw that knockdown of β3 integrin can cause increase of αvβ5 integrin which is a limiting factor for Ad5-mediated gene transfer and consequently increase transduction efficiency [26]. Thus, it is possible that knockdown of β3 integrin increased expression of some other integrins that caused increased binding of AdFNGR and AdHNGR, but this increased binding did not result in increased transduction efficiency. Contrary to αvβ3 integrin, CD13 knockdown did not have any effect on transduction efficiency of AdFNGR on RD and caused modest decrease in transduction efficiency of AdFNGR in SLK cell line. This further supports our conclusion that at least for the cell lines in this study, the major retargeting receptor for AdFNGR is αvβ3 integrin and not CD13. To our surprise, decreased expression of either αvβ3 integrin or CD13 had no effect on transduction efficiency of AdHNGR in SLK cell line. We hypothesize that there is a certain threshold in CD13 and αvβ3 integrin amount that is needed for efficient NGR-retargeting of AdFNGR and AdHNGR, respectively. Since SLK are 100% positive for both CD13 and αvβ3 integrin expression and siRNA mediated knockdown did not completely eliminate the expression of these molecules, we believe that threshold in CD13/αvβ3 integrin was not reached causing no change in AdFNGR and AdHNGR transduction efficiency. Based on data obtained on RD and MDA-MB-435S cell lines we propose that αvβ3 integrin plays major role in AdFNGR retargeting. However, we cannot conclude which of CD13 and αvβ3 integrin is more important for AdHNGR retargeting potential.

Opposite to this finding, in our previous work we showed that disulfide bond formation within an Ad5 bearing the CDCNGRCFC sequence in HI loop of fiber protein is essential for retargeting to CD13, suggesting that this sequence does indeed assume a cyclic

structure which facilitates NGR binding to CD13 [13]. However, Ad5NGR4C and AdFNGR bear different NGR targeting sequences, CDCNGRCFC and CNGRCVSGCAGRC respectively, which further underlines that NGR flanking sequences can influence receptor selectivity.

Recently NGR-tagged gold nanoparticles have been proposed as a novel platform for drug delivery to tumor endothelial cells for cancer therapy. Mechanistic studies confirmed that a primary mechanism of NGR tagged gold nanoparticles cell entry was CD13 targeting and excluded a major role of integrin targeting as a consequence of NGR deamidation, i.e. generating isoDGR integrin ligand [30] which is different from the results we obtained in this study. However, one has to keep in mind that steric conformation of NGR peptides inserted into the adenovirus capsid proteins will be influenced by the entire adenovirus particle, while chemical preparations of peptides containing NGR embedded in different scaffolds could be easier controlled. For example, AdHNGR has 720 NGR-retargeting motifs per virus particle in comparison to 36 for AdFNGR, which is why changes in expression of adenovirus receptors might affect differently AdHNGR than AdFNGR. Of note, different CD13 isoforms are expressed within tumor vessels, normal epithelia, and myeloid cells which can further explain differences in NGR binding affinity between the CD13 expressed *in vivo* by tumor vessels and the CD13 form expressed by cells in *in vitro* studies [31].

Conclusion

In this study we investigated the role of different adenovirus insertion sites, namely fiber and hexon, on retargeting properties of NGR-modified AdFNGR and AdHNGR. We propose that NGR peptide inserted into the fiber protein of AdFNGR can undergo NGR-to-isoDGR change which further on influences its retargeting towards αvβ3 integrin. Contrary, hexon protein as an insertion moiety does not allow circularization of inserted peptide therefore leaving NGR sequence of AdHNGR in the linear form. We could not distinguish which of CD13 and αvβ3 integrin is more important for AdHNGR retargeting potential, however in our molecular model we did identified possible penetration site for NGR peptide in CD13 protein. In conclusion, molecular scaffold of NGR targeting peptide is critical for their receptor binding affinity/specificity and biological activity *in vitro* not only for NGR-containing peptides themselves [5, 32] but also for viral vectors bearing NGR-containing peptides aimed at targeting tumor vasculature.

Highlights

- AdFNGR and AdHNGR bind better to CD13 and/or αvβ3 integrin-positive cells than Adwt.
- Reducing disulfide bonds by using dithiothreitol decreased transduction efficiency and binding of both AdFNGR and AdHNGR.
- Mass spectrometry analysis done on purified viruses indicate that cysteins from CNGRCVSGCAGRC peptide within AdHNGR do not form disulfide bonds.
- Retargeting properties of AdFNGR and AdHNGR rely mainly on αvβ3 integrin expression.

Acknowledgment

The authors would like to thank Ms Marina Šutalo for her technical assistance.

Funding

This work was partly supported by the Croatian Science Foundation postdoctoral grant to DM.

Authorship Contributions

Conceptualization, D.N., A.AR, K.B. and D.M.; methodology, D.N., A.H., Z.B., M.C., A.B., B.J., K.P; writing—original draft preparation, D.M.; writing—review and editing, D.N., A.AR, K.B; supervision, D.M.; project administration, D.M.; funding acquisition, D.M.

Conflict of interest statement

The authors declare no conflict of interest.

Literature

1. Arap, W., R. Pasqualini, and E. Ruoslahti, *Cancer Treatment by Targeted Drug Delivery to Tumor Vasculature in a Mouse Model.* Science, 1998. **279**(5349): p. 377.
2. Pasqualini, R., et al., *Aminopeptidase N is a receptor for tumor-homing peptides and a target for inhibiting angiogenesis.* Cancer Research, 2000. **60**(3): p. 722-727.
3. Corti, A. and F. Curnis, *Isoaspartate-dependent molecular switches for integrin-ligand recognition.* J Cell Sci, 2011. **124**(Pt 4): p. 515-22.
4. Curnis, F., et al., *Spontaneous formation of L-isoaspartate and gain of function in fibronectin.* Journal of Biological Chemistry, 2006. **281**(47): p. 36466-36476.
5. Curnis, F., et al., *Critical Role of Flanking Residues in NGR-to-isoDGR Transition and CD13/Integrin Receptor Switching.* Journal of Biological Chemistry, 2010. **285**(12): p. 9114-9123.
6. Corti, A., et al., *The neovasculature homing motif NGR: more than meets the eye.* Blood, 2008. **112**(7): p. 2628-35.
7. Corti, A., et al., *NGR-TNF Engineering with an N-Terminal Serine Reduces Degradation and Post-Translational Modifications and Improves Its Tumor-Targeting Activity.* Molecular Pharmaceutics, 2020. **17**(10): p. 3813-3824.
8. Colombo, G., et al., *Structure-activity relationships of linear and cyclic peptides containing the NGR tumor-homing motif.* Journal of Biological Chemistry, 2002. **277**(49): p. 47891-47897.

9. Gregorc, V., et al., *NGR-hTNF in combination with best investigator choice in previously treated malignant pleural mesothelioma (NGR015): a randomised, double-blind, placebo-controlled phase 3 trial.* Lancet Oncol, 2018. **19**(6): p. 799-811.
10. Gai, Y., et al., *Evaluation of an Integrin αvβ3 and Aminopeptidase N Dual-Receptor Targeting Tracer for Breast Cancer Imaging.* Molecular Pharmaceutics, 2020. **17**(1): p. 349-358.
11. Liu, L.Q., et al., *Incorporation of tumor vasculature targeting motifs into moloney murine leukemia virus Env escort proteins enhances retrovirus binding and transduction of human endothelial cells.* Journal of Virology, 2000. **74**(11): p. 5320-5328.
12. Grifman, M., et al., *Incorporation of tumor-targeting peptides into recombinant adeno-associated virus capsids.* Molecular Therapy, 2001. **3**(6): p. 964-975.
13. Majhen, D., et al., *Disulfide bond formation in NGR fiber-modified adenovirus is essential for retargeting to aminopeptidase N.* Biochem Biophys Res Commun, 2006. **348**(1): p. 278-87.
14. Jullienne, B., et al., *Efficient delivery of angiostatin K1-5 into tumors following insertion of an NGR peptide into adenovirus capsid.* Gene Ther, 2009. **16**(12): p. 1405-15.
15. Luisoni, S. and U.F. Greber, *2 - Biology of Adenovirus Cell Entry: Receptors, Pathways, Mechanisms A2 - Curiel, David T*, in *Adenoviral Vectors for Gene Therapy (Second Edition)*. 2016, Academic Press: San Diego. p. 27-58.
16. Barry, M.A., J.D. Rubin, and S.C. Lu, *Retargeting adenoviruses for therapeutic applications and vaccines.* FEBS Lett, 2020. **594**(12): p. 1918-1946.
17. Majhen, D., et al., *The disulfide bond of an RGD4C motif inserted within the Hi loop of the adenovirus type 5 fiber protein is critical for retargeting to alpha(v)-integrins.* Journal of Gene Medicine, 2012. **14**(12): p. 788-797.
18. Mittereder, N., K.L. March, and B.C. Trapnell, *Evaluation of the concentration and bioactivity of adenovirus vectors for gene therapy.* Journal of Virology, 1996. **70**(11): p. 7498-7509.
19. Majhen, D., et al., *Increased Adenovirus Type 5 Mediated Transgene Expression Due to RhoB Down-Regulation.* Plos One, 2014. **9**(1).
20. Maier, J.A., et al., *ff14SB: Improving the Accuracy of Protein Side Chain and Backbone Parameters from ff99SB.* Journal of Chemical Theory and Computation, 2015. **11**(8): p. 3696-3713.
21. Tomić, A., et al., *New Zinc Ion Parameters Suitable for Classical MD Simulations of Zinc Metallopeptidases.* Journal of Chemical Information and Modeling, 2019. **59**(8): p. 3437-3453.
22. Joung, I.S. and T.E. Cheatham, 3rd, *Determination of alkali and halide monovalent ion parameters for use in explicitly solvated biomolecular simulations.* J Phys Chem B, 2008. **112**(30): p. 9020-41.
23. Darden, T., D. York, and L. Pedersen, *Particle mesh Ewald: An N·log(N) method for Ewald sums in large systems.* The Journal of Chemical Physics, 1993. **98**(12): p. 10089-10092.
24. Abraham, M., et al., *the GROMACS development team, GROMACS User Manual version 2018*. 2018.
25. Majhen, D., et al., *Increased expression of the coxsackie and adenovirus receptor downregulates alphavbeta3 and alphavbeta5 integrin expression and reduces cell adhesion and migration.* Life Sci, 2011. **89**(7-8): p. 241-9.
26. Stojanović, N., A. Dekanić, and M. Paradžik, *Differential Effects of Integrin αv Knockdown and Cilengitide on Sensitization of Triple-Negative Breast Cancer and Melanoma Cells to Microtubule Poisons.* 2018. **94**(6): p. 1334-1351.
27. Samaržija, I. and A. Dekanić, *Integrin Crosstalk Contributes to the Complexity of Signalling and Unpredictable Cancer Cell Fates.* 2020. **12**(7).
28. Humphrey, W., A. Dalke, and K. Schulten, *VMD: Visual molecular dynamics.* Journal of Molecular Graphics, 1996. **14**(1): p. 33-38.

29. Lu, X., et al., *Deamidation and isomerization liability analysis of 131 clinical-stage antibodies.* 2019. **11**(1): p. 45-57.
30. Curnis, F., et al., *NGR-tagged nano-gold: A new CD13-selective carrier for cytokine delivery to tumors.* Nano Res, 2016. **9**(5): p. 1393-1408.
31. Curnis, F., et al., *Differential binding of drugs containing the NGR motif to CD13 isoforms in tumor vessels, epithelia, and myeloid cells.* Cancer Res, 2002. **62**(3): p. 867-74.
32. Corti, A., et al., *Glycine N-Methylation in NGR-Tagged Nanocarriers Prevents Isoaspartate Formation and Integrin Binding without Impairing CD13 Recognition and Tumor Homing.* Advanced Functional Materials, 2017. **27**(36).

Authorship Contributions

Conceptualization, D.N., A.AR, K.B. and D.M.; methodology, D.N., A.H., Z.B., M.C., A.B., B.J., K.P; writing—original draft preparation, D.M.; writing—review and editing, D.N., A.AR, K.B; supervision, D.M.; project administration, D.M.; funding acquisition, D.M.